CHEMISTRY
A EUROPEAN JOURNAL

DOI: 10.1002/chem.201100854

Dynamics of the Glycosidic Bond: Conformational Space of Lactose

Máté Erdélyi,[a, b] Edward d′Auvergne,[a] Armando Navarro-Vázquez,[c] Andrei Leonov,[a] and Christian Griesinger*[a]

Abstract: The dynamics of the glycosidic bond of lactose was studied by a paramagnetic tagging-based NMR technique, which allowed the collection of an unusually large series of NMR data for a single compound. By the use of distance- and orientation-dependent residual dipolar couplings and pseudocontact shifts, the simultaneous fitting of the probabilities of computed conformations and the orientation of the magnetic susceptibility tensor of a series of lanthanide complexes of lactose show that its glycosidic bond samples *syn*/*syn*, *anti*/*syn* and *syn*/*anti* ϕ/ψ regions of the conformational space in water. The analysis indicates a higher reliability of pseudocontact shift data as compared to residual dipolar couplings with the presently available weakly orienting paramagnetic tagging technique. The method presented herein allows for an improved understanding of the dynamic behaviour of oligosaccharides.

Keywords: glycosidic bonds · molecular dynamics · NMR spectroscopy · oligosaccharides · paramagnetism

Introduction

Molecular recognition processes commonly involved in vital enzymatic and immunorecognition functions[1] are frequently mediated by protein–oligosaccharide interactions.[2] Such processes are exceedingly sensitive to the structure and dynamics of the interaction partners,[3] as exemplified by the selective binding of terminal lactose units of glycoproteins by the highly cytotoxic herbal protein ricin.[4] The geometry and conformational flexibility of saccharides in general and specifically of lactose have over the past decades been assessed by a range of computational,[5] crystallographic,[6,7] NMR spectroscopic[8] and combined theoretical and spectroscopic techniques.[9,10] Molecular dynamics (MD) simulation proposed flexibility and five low-energy regions on the potential energy map of the glycosidic bond, whereas NMR spectra and X-ray crystallography converged to the almost exclusive existence of a single, well-defined conformation with *syn*-ψ/*syn*-ϕ glycosidic geometry. Notably, these techniques are often inadequate for the reliable determination of the structure of saccharides because computations suffer from parameterisation dependency,[11] whereas conventional *J*- and NOE-based NMR techniques are hampered by recurrent signal overlaps and the limited number of available inter-residual restraints in saccharides as well as by the possible overestimation of short distances yielding virtual conformations.[12] The limitations of X-ray crystallography for reflecting highly dynamic solution structures are known.[13] A recent combined residual dipolar coupling (RDC) and MD-based approach validated the single conformation minimum of lactose found by X-ray crystallography.[9,10] However, through a thorough NMR investigation we reveal that, in agreement with MD predictions,[5] the glycosidic bond of lactose is mobile and the X-ray conformation is only one of several geometries present in solution.

[a] Dr. M. Erdélyi, Dr. E. d′Auvergne, Dr. A. Leonov, Prof. C. Griesinger
NMR-Based Structural Biology
Max Planck Institute for Biophysical Chemistry
Am Fassberg 11, 37077 Göttingen (Germany)
Fax: (+49) 551-201-2202
E-mail: cigr@nmr.mpibpc.mpg.de
Homepage: http://medusa.nmr.mpibpc.mpg.de/

[b] Dr. M. Erdélyi
Department of Chemistry and the Swedish NMR Centre
University of Gothenburg (Sweden)

[c] Dr. A. Navarro-Vázquez
Department of Organic Chemistry
Universidade de Vigo (Spain)

Supporting information for this article is available on the WWW under http://dx.doi.org/10.1002/chem.201100854.

Results and Discussion

Paramagnetically induced RDCs and pseudocontact shifts (PCSs) have been shown to be useful to quantify interdomain motions of proteins.[14–16] It was shown that only one set of signals is observed with ethylenediaminetetraacetic acid (EDTA)-type tags.[16] Here, this approach is transferred to the study of the motion of diamagnetic saccharides, such as lactose, by converting them to paramagnetic compounds through attachment of an EDTA-based paramagnetic tag as depicted in Figure 1.[16] Based on our experience with protein tags,[15–17] the lanthanide chelating unit was rigidly connected with lactose through a biphenyl moiety. This linker not only keeps the tag at a defined distance long enough to minimise paramagnetic relaxation of the NMR signals of lactose, but also implements a spacer with a single axis of

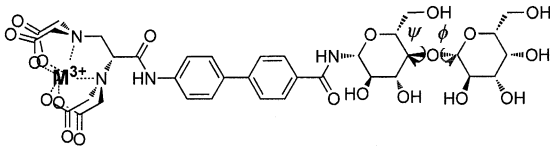

Figure 1. Paramagnetically tagged lactose, in which M^{3+} can be any lanthanide. Herein the lanthanides Dy^{3+}, Tb^{3+}, Tm^{3+}, Er^{3+}, Eu^{3+} and Yb^{3+} were employed.

rotation thereby minimising the orientational averaging of RDCs and PCSs (Figure 2) as well as simplifying its mathematical treatment.

When domain motion in proteins is characterised by paramagnetic tagging, a sufficient number of anisotropic restraints can normally be measured for the determination of alignment tensors for the two or more domains under investigation. For saccharides, this is not the case and therefore we chose an alternative approach based on cross validation of selections of complete ensembles covering all theoretically possible conformations generated by Monte Carlo conformational search against the anisotropic parameters. Ensembles covering energies within 42 kJ mol^{-1} were generated by a Monte Carlo conformational search using the OPLS-2005 force field[18,19] and the generalised Born/solvent-accessible surface area (GB/SA) water solvation model[20] as implemented in the program MacroModel.[21] The copious energy window applied herein ensured full coverage of the conformational space of the glycosidic bond of lactose. To avoid over-fitting, 15 geometries representative of the low-energy regions of the potential energy map[5] were selected out of 637 generated conformations (S1, Supporting Information). The 15 geometries faithfully represent the ensemble of lactose (Supporting Information).

To achieve the highest possible reliability in the determination of the conformational ensemble of lactose, we measured PCSs and RDCs by using six different trivalent lanthanide ions, Dy^{3+}, Tb^{3+}, Tm^{3+}, Er^{3+}, Eu^{3+} and Yb^{3+} (values given in the Supporting Information), by referencing against diamagnetic La^{3+} recorded with a standard *F*2-coupled HSQC[22] to give ^1J(C,H) in the well-sampled, directly observed ^{1}H dimension. Use of the La^{3+} complex as reference is valid because of the similar ionic radii of lanthanides. For cross validation, we assumed that each lanthanide induces a single time-averaged alignment tensor $\mathbf{A}_i$ independent of the conformational flexibility of the lactose ensemble.[23] This assumption relies on the independence of internal motion of the sugar from the internal motion of the tag. Due to the distance (16.5 Å) between the lanthanide and the sugar, the specific conformation of the sugar does not affect the magnetic susceptibility of the tag, hence it does not influence alignment and therefore a multiple alignment tensor approach would not be required for this system. Consequently, throughout the computational fitting of the NMR data to the ensemble, all structures were superimposed at the NH of the interconnecting amide bond and the C1 and C2 positions of glucose, as these are the sugar atoms exhibiting the least amount of motion relative to the alignment-inducing lanthanide.

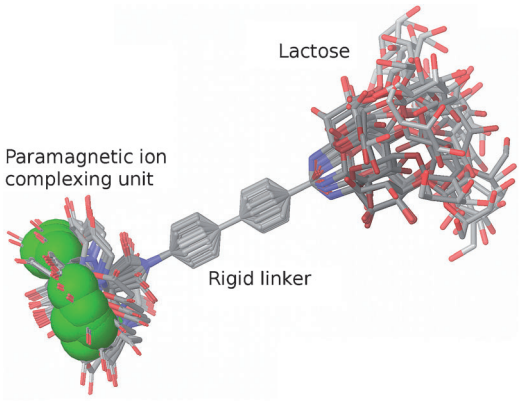

Figure 2. Overlaid conformations of lactose connected to a paramagnetic centre through a rigid biphenyl–EDTA-type paramagnetic tag, which allows rotation only around a single axis and keeps the paramagnetic centre (green) at a well-defined distance from the saccharide to control paramagnetic relaxation-induced line broadening. The structures were generated by using a systematic Monte Carlo conformational search with the program MacroModel.

For the cross validation of ensembles against the measured PCSs, we used Equation (1)

$$\delta_{ij}(\theta) = \sum_{c=1}^{N} p_c \frac{\mu_0}{4\pi} \frac{15kT}{B_0^2} \frac{1}{r_{jc}^3} \mu_{jc}^T \mathbf{A}_i \mu_{jc} \qquad (1)$$

in which N is the total number of states or structures, p_c is the weight or probability associated with conformation c, μ_0 is the permeability of vacuum, k is Boltzmann's constant, T is the absolute temperature, B_0 is the magnetic field strength, r_{jc} is the distance between the paramagnetic centre used for alignment condition i and the nuclear spin j, μ_{jc}^T is the unit row-vector between the metal and spin j in conformation c, and $\mathbf{A}_i$ is the alignment tensor for alignment condition i. The location of the metal centre was approximated by a single position due to the long distance between the sugar and the metal (see below). For the RDC between spins j and l, Equation (2)

$$D_{ijl} = -3 \frac{1}{2\pi} \frac{\mu_0}{4\pi} \frac{\gamma_j \gamma_l \hbar}{r_{jl}^3} \sum_{c=1}^{N} p_c \mu_{jlc}^T \mathbf{A}_i \mu_{jlc} \qquad (2)$$

was applied, in which D_{ijl} is the dipolar coupling constant in Hertz in alignment condition i and μ_{jlc}^T is the unit vector between spins j and l in conformation c. The formulae and analyses were implemented in the program relax[24] as described in the Supporting Information.

RDCs and PCSs for all six alignments—induced by the various paramagnetic lanthanides—were used to simultaneously optimise all six alignment tensors and the probability of each member of the ensemble. Thus, one of the main advantages of the applied method is that it allows for the description of the conformational ensemble of a single com-

pound by using six different sets of data. Taking into consideration the well-known rigidity of pyranoid sugar units resulting in the nearly exclusive existence of their chair conformations,[25] the major cause of the flexibility of lactose is dynamics about its glycosidic bond, which herein is described by an unusually large number of experimental data. The standard chi-squared statistic target function was applied in the optimisation [Eq. (3)]

$$\chi^2 = \sum_i \frac{(D_i - D_i(\theta))^2}{\sigma_i^2} \tag{3}$$

in which D_i is the measured RDC or PCS, $D_i(\theta)$ is the back-calculated RDC or PCS, and σ_i is the corresponding experimental error. The experimental temperature of 298 K and magnetic field strength of 21.1 T (^{1}H 900 MHz) were used in the computations. Due to under-representation of the mobility in the small selections of conformations or single structures used here for comparison (Table 1), the RDCs for the saccharide CH_2 groups and the PCSs of their protons were excluded from the optimisation. The CH bond length was set to 1.10 Å. Validated by the large separation between the metal and the sugar, and by the independence of tag and sugar motions, an average lanthanide position determined by 1000 Monte Carlo samplings of the tag was used in the calculation. For the PCSs, it is an approximate but valid assumption because the tag is sufficiently far away from the sugar that its motion only marginally affects the lanthanide–nuclear spin distance and the orientation of this vector with respect to the alignment tensor.

Table 1. Qualities of the fits of the published structures and the ensembles computed throughout this study to the experimentally observed PCSs and RDCs originating from six different alignments induced by different lanthanides.

Entry	Structure/ensemble	k[a]	Q_{PCS}	Q_{RDC}[b]	AIC[c]
1	MD/NMR[9]	560	0.281	0.626	2538.1
2	NMR (NOE)[8]	60	0.285	0.575	1674.2
3	X-ray[6]	60	0.284	0.558	1605.5
4	X-ray[7]	60	0.264	0.391	1132.5
5	MD, lowest-energy structure[5]	60	0.288	0.603	1806.6
6	in vacuo energies[5]	60	0.317	0.431	2144.0
7	aqueous energies[5]	60	0.302	0.410	1962.0
8	Monte Carlo conformational search	74	0.248	0.502	847.6

[a] The parameter number (the 60 tensor components together with the weights for each member of the ensemble). [b] Note that the Q_{RDC} should not be used for comparison of the quality of the structural ensembles, as explained in the text. [c] Akaike's Information Criterion for comparing the models.

Q factors for RDCs were calculated following the Pales definition,[26] whereas Q factors for the PCSs were defined as [Eq. (4)]

$$Q = \sqrt{\frac{\sum_i (D_i - D_i(\theta))^2}{\sum_i D_i^2}} \tag{4}$$

Ensembles were compared based on the value of the Akaike's Information Criterion (AIC),[27] the gold standard statistical criterion for model selection. This belongs to the frequentist methods, which is one of the three major pillars of statistics besides hypothesis testing (analysis of variance (ANOVA) statistics) and Bayesian methods.[28] By using this, the model showing the lowest criterion value is considered to best reproduce reality, here meaning the structure or ensemble closest reflecting the properties of lactose as described by the experimental data. This method permits a comparison of dynamics of small flexible molecules based on experimental observation, instead of using computational MD simulations. The Akaike criterion for our experimental data was derived on the assumption of Gaussian errors for the RDC and PCS values as [Eq. (5)]

$$\mathrm{AIC} = \chi^2 + 2k \tag{5}$$

in which k is the total number of alignment tensor and population member weight parameters.[29]

The lowest PCS Q factor and the by far lowest AIC value (Table 1) indicate that the ensemble derived by Monte Carlo conformer search sampling of the full conformational space (Table 1, entry 8) provides a significantly better description of lactose in aqueous solution than any of the previously proposed structures that were derived from X-ray, NMR or computational investigations. In contrast to the previous studies of Table 1, entries 1–5, this ensemble (Table 1, entry 8) reveals that lactose may not exclusively adopt a *syn*-ψ/*syn*-ϕ conformation at its glycosidic bond, but samples a number of low-energy regions which, along with their estimated probabilities, are shown in Figure 3. *syn* torsion angles range from −60° through 0° to +60° and *anti* from −120° through 180° to +120°. The populations of the various ψ/ϕ combinations are listed in Table S1 (Supporting Information). The population-averaged (Table 1, entry 8) glycosidic H1′–H4 distance (2.6 Å) is in excellent agreement

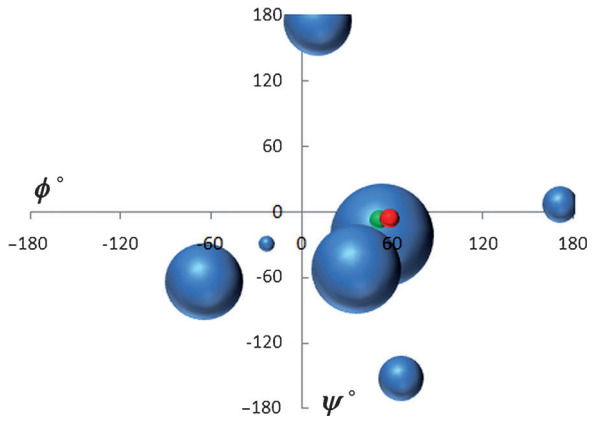

Figure 3. The ϕ,ψ plot representing the glycosidic linkage of lactose. The best ensemble (Table 1, entry 8) is shown with the size representing the weight of the conformation. Previous X-ray[7] and NMR-derived[9] structures are shown in green and red, respectively. The actual values and dihedral angles are given in the Supporting Information.

with the measured value (2.5 Å, NOE).[9,30] Despite the larger number of parameters of the Monte Carlo-derived conformational ensemble (Table 1, entry 8), its statistics indicate that the ensemble is not over-fit and is significantly better than the previously published structures. The AIC model selection criterion better reflects the quality of fit of the ensembles and single structures than the unrelated and commonly reported PCS Q factor. The reason is that AIC considers and penalises over-fitting whereas the Q factor does not. The ensembles have more parameters than the single structures and could fit the experimental data with lower Q factors by absorbing experimental noise even if a single conformation were to be present in aqueous solution. The AIC value ensures that the ensemble and single structures have equal footing in the comparison. It should also be emphasised that the RDC Q factors of all available models are unreasonable and therefore cannot be used for comparison. The reason for this is the low orienting ability of the presently available paramagnetic tags, which yield an order of magnitude smaller RDCs than those usually induced by external alignment media (10–40 Hz).[31] PCSs, unavailable in external orienting media, are one to two orders of magnitude larger than the RDCs and therefore less affected by the intrinsic error of the measurement technique.

Due to the proton–proton coupling pattern unavoidably present in the HSQC cross peaks, multiple measures of both the chemical shifts and the coupling constants were possible. For example, when a ^1J(C,H) doublet of ^3J(H,H) triplets is observed in a coupled ^{1}H,^{13}C HSQC spectrum, there are six possibilities for measurement of the carbon chemical shift, three of the proton chemical shift as well as three of the J or $J+D$ values. Applying the standard deviation formula and quadratic averaging, error estimates were derived from both the diamagnetic La^{3+} complex reference spectrum and from the spectrum of the paramagnetic Yb^{3+} complex. To obtain error estimates for peak positions, these two errors were quadratically averaged. Originating from the nature of the measurement, for PCSs which are shift differences, the obtained variances were doubled whereas for the RDCs which are differences of shift differences, the variances were quadrupled yielding estimated errors of $\sigma_{RDC}=2.36$ Hz, $\sigma_{^{13}CPCS}=0.0267$ ppm and $\sigma_{^1HPCS}=0.00268$ ppm.[32] Although additional sources of errors such as those originating from residual chemical shift anisotropy (rCSA) cannot be excluded, these values are in good agreement with previous data.[33] As the rCSA is observed as a change in chemical shift, it only affects the PCS measurements and not the RDC. Therefore, it was taken into account in this analysis by an additional error equal to the maximal change in rCSA-induced chemical shift, of magnitude comparable to that reported for saccharides in the literature.[33] The rCSA is the largest if the main axis of the CSA tensor is parallel to the main axis of the alignment tensor. As the optimised alignment tensors have an axial component A_a of 2×10^{-4} on average (the fitted values range from 5×10^{-4} to -1×10^{-4} for the structures in Table 1), the absolute maximum rCSA value was calculated by using Equation (6).

$$\max \mathrm{rCSA} = A_a \times \delta_{axial} \quad (6)$$

Thus, for lactose protons with reported CSAs of 2 to 6 ppm,[33a] the average value of 4 ppm provides a maximum rCSA value of 0.0008 ppm, which is approximately four times smaller than the experimental noise. Carbon atoms with reported CSA ranging from 30 to 60 ppm[33b] may have a maximal rCSA of 0.012 ppm, which is half the magnitude of the approximate measurement error in the indirectly observed dimension. These rCSA error estimates are comparable to those reported in the literature[33] and because they were smaller than the experimental errors, they were incorporated in the calculation as an added error to the experimental error, estimated as described above. Because of the use of a chi-squared optimisation target function and the comparatively large errors of the RDCs and of ^{13}C PCSs, as shown in the correlation plots of the fitted versus the measured data in Figure 4, they had a smaller influence on the orientation and the conformational selection in the current analysis. This measurement error is well reflected by the large RDC Q factors (Table 1) and the subsequent bad fit of

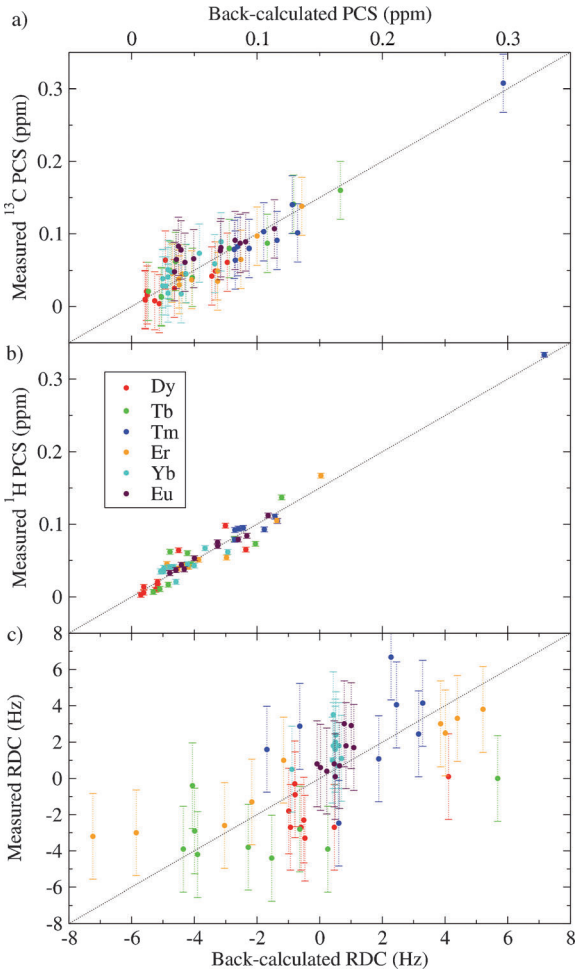

Figure 4. PCS and RDC correlation plots: a) ^{13}C PCS, b) ^{1}H PCS, and c) RDC. These correlation plots correspond to the best solution of the Monte Carlo conformer ensemble.

the RDC data (Figure 4). The method would further benefit from an increase in the degree of alignment resulting in amplified RDCs and PCSs. As these measurements were performed on a 900 MHz spectrometer, increasing the B_0 field strength significantly to further increase the degree of alignment is currently not possible. For the achievement of the largest possible RDCs, the strongest aligning lanthanides were used in the analysis.[34] Future advancements in alignment strength would be beneficial for such RDC- and PCS-based studies on the dynamics of small molecules.

We showed that the ensemble corresponding to entry 8 in Table 1 fits the experimental data best. The optimisation space is complex, consisting of numerous local minima. Therefore multiple optimisations starting from random positions in the space were applied to probe and search for the global minimum (the relax script used for this analysis is given in the Supporting Information). The global minimum consisted of 75 and 4% *syn*-ϕ/*syn*-ψ and *anti*-ϕ/*syn*-ψ orientations, respectively, and 20% for the *syn*-ϕ/*anti*-ψ geometry of the glycosidic bond (Table 1, entry 8; Figure 3; populations listed in Table S1 in the Supporting Information). These probabilities closely match the potential energy surface map of lactose determined by Oh et al.[5] Yet when conformations corresponding to the energy minima of the in vacuo and aqueous environments are weighted by the computed Boltzmann energies, neither of these accurately reproduce the data (Table 1, entries 6 and 7). The poor fit of these ensembles is well explained by the known uncertainties of the energies of conformations derived by computation.[35] Such methods provide ensembles encompassing the geometries present in solutions along with a large number of additional, theoretically possible conformations, which in reality may have zero probabilities.[36] Hence, theoretical conformational pools allow the identification of solution geometries when utilised in combination with even sparse experimental data.[36–40] The AIC and Q_{PCS} values of the X-ray structures of lactose (Table 1, entries 3 and 4)[6,7] that are considerably higher than those of Table 1, entry 8, confirm that the geometry preferred in the solid state, and also found to be dominant in solution, is by itself incapable of describing the full range of conformations of lactose in solution. The PCS data we have measured do not fit to the single structure representation. The AIC and Q_{PCS} statistical indicators of the combined computational and NMR-derived structure (Table 1, entry 1) published by Jiménez-Barbero et al.[9] show that, despite the high probability of the *syn*-ϕ/*syn*-ψ orientation of the lactose glycosidic bond in solution, this orientation is not exclusively present in solution. It should be emphasised that the energetically preferred conformation of lactose was well identified by the RDC-based studies using external alignment;[8,9] however, these methods appear inferior for the detection of dynamics, that is, the identification of minor conformers as compared to the technique presented here. As the bioactive conformation of small molecules does not necessarily correspond to the structure energetically most preferred in solution, yet is expected to be present to a measurable extent among those populated in their solution ensemble,[39,41] the identification of minor conformers is of great importance, especially for oligosaccharides which are known to mediate vital molecular recognition processes.[1]

Conclusion

The presented RDC- and PCS-based ensemble analysis reveals a spread of orientations along the glycosidic bond of lactose in an aqueous environment, which is in excellent agreement with the predictions of MD simulations.[5] Even though populations of the conformations could only be defined to lie within certain ranges by our analysis, we can exclude that lactose exists in solution in a single rigid conformation as proposed in all experimental studies.[9,10] NMR techniques using external alignment might be less applicable for studying dynamics as in aligned solutions the alignment tensor varies with conformation, thus limiting the applicability of this approach by approximations, which are unlikely to be valid for small organic molecules. By using the tagging methodology the attached paramagnetic tag is far away from the investigated glycosidic linkage and therefore has no significant effect on its behaviour, as confirmed by the comparable predicted dihedral angles of lactose and tagged lactose (Figure S1, Supporting Information). The population-averaged (Table 1, entry 8) glycosidic H1′–H4 distance (2.6 Å) is in good agreement with that derived from NOE measurements.[9,30] Our results demonstrate that the applied paramagnetic tagging-based technique allows for the description of the motion of the glycosidic linkage in lactose and more generally in saccharides. It permits the collection of several complementary series of RDC and PCS data of the same ensemble by simple variation of the complexed paramagnetic ion. The increased number of available experimental parameters provides greatly improved reliability for the investigation of dynamic processes. In a related study, we demonstrated for the example of *N*,*N*-diacetylchitobiose[42] that the applied paramagnetic tagging technique is capable of identifying rigid glycosidic linkages of sugars, and thereby have proven that this approach is capable of differentiating between rigid and dynamic glycosidic bonds.

Experimental Section

NMR experiments: Measurements were carried out on Bruker 400 and 900 MHz spectrometers. Resonance assignment was performed by using HSQC, HMBC, exclusive correlation spectroscopy (E.COSY), TOCSY and NOESY experiments. For detection of RDCs and PCSs, the lanthanide complexes of the tagged lactose were investigated with HSQC-type experiments, as implemented in the program TopSpin and given in the Supporting Information (S7), thereby providing heteronuclear couplings in the directly detected dimension. It should be noted that in principle any coupled HSQC pulse sequence could be applied for acquisition of such spectra. The choice of this particular pulse program[22a,c,d] with adiabatic pulses for broad-band carbon inversion and refocusing, a heteronuclear gradient echo and sensitivity enhancement (preservation of equivalent pathways, PEP) is optimal for molecules in natural abundance to

remove artefacts. In similarity to previous studies,[43] the HSQC spectra were acquired at the highest field available in our laboratory (900 MHz) to minimise second-order effects on splitting of ring protons. The relaxation delay ($d1$) was set to 2.0 s; 16 scans were accumulated, and 4096 and 512 points were acquired in the direct and indirect dimensions, respectively. The spectral width was set to 7183.9 (^{1}H) and 2264.4 Hz (^{13}C) and the temperature was regulated at 298 K. The acquisition time was ≈0.3 s, and the spectrometer frequency 899.73 and 226.24 MHz in the ^{1}H and ^{13}C dimensions, respectively. The spectra were processed using zero filling to 8192×4096 points, and the selected increments converted by inverse Fourier transformation to one-dimensional free induction decays (FIDs), which in turn were processed by zero filling to 16384 points.

The tagged lactose was dissolved in 4-(2-hydroxyethyl)-1-piperazineethanesulfonic acid ([D_{18}]HEPES) buffer solution (0.1 M, pH 8) prepared with D_2O as solvent and CH_3CN (5 μL) added as chemical shift reference. The solution was then titrated with an aqueous [D_{18}]HEPES (0.1 M) solution of MCl_3 (M: a lanthanide(III) ion) until the signals of the non-complexed compound completely disappeared. Exact quantities of each component of the final solution were added through the application of stock solutions of each component. RDCs were obtained by subtracting the ^1J(C,H) value obtained for the La^{3+} complex from the (^1D-(C,H)+^1J(C,H)) value measured for a paramagnetic complex (Dy^{3+}, Tb^{3+}, Tm^{3+}, Er^{3+}, Yb^{3+} or Eu^{3+}). PCSs were measured as the chemical shift differences of the corresponding peaks in the referenced (CH_3CN), overlapped spectra of the oriented and non-oriented solutions. The total volume of the solution studied in Shigemi tubes was 300 μL and contained 1.8 mg (2.1 μmol) sugar. Spectral processing was performed with the software TopSpin. Coupling constants were read by selecting the corresponding traces in the 2D HSQC spectra, performing a reverse Fourier transformation and saving the FID of the trace. This FID was zero-filled to 16384 points, which resulted in a digital resolution of 0.4 Hz. Couplings were then read by manual J-doubling.[44]

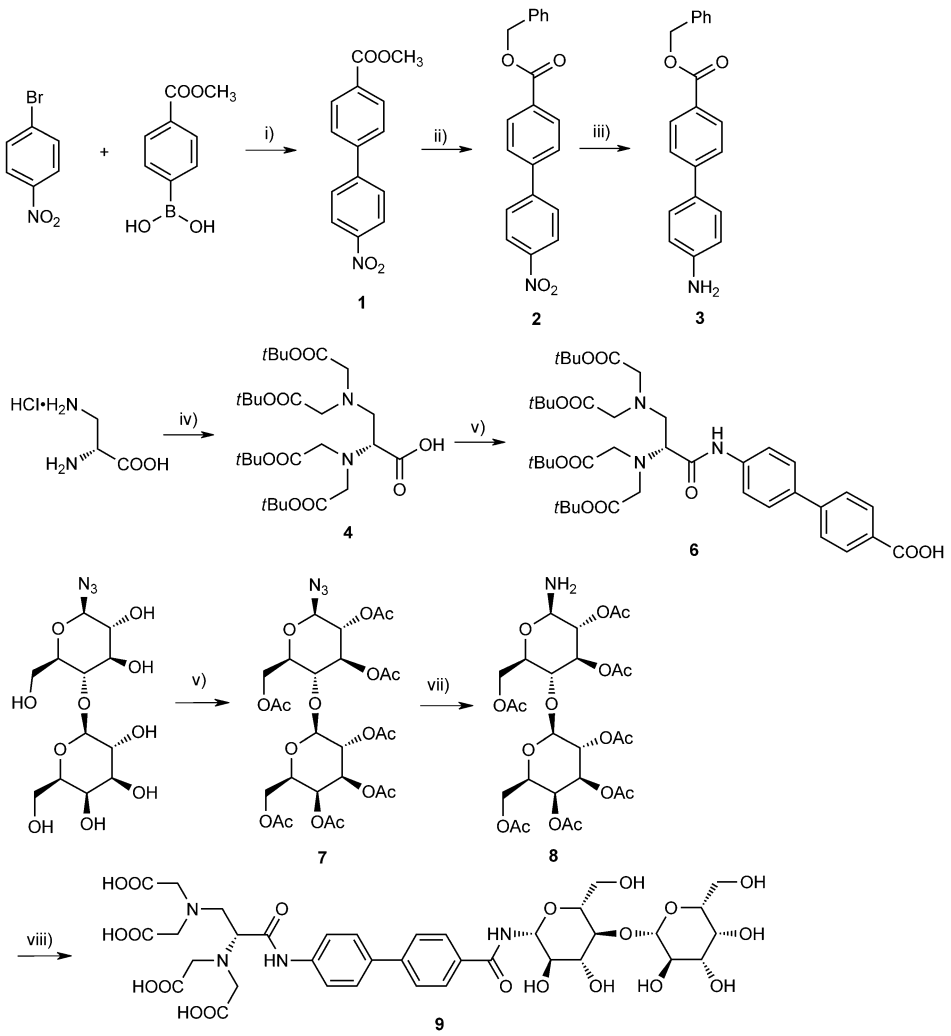

Scheme 1. Outline of the synthesis of paramagnetically labelled lactose. Conditions: i) [$Pd(PPh_3)_2Cl_2$], DME, aqueous Na_2CO_3, 90 °C, 5 h, 72 %; ii) [$Ti(OC_3H_7)_4$], $PhCH_2OH$, 150 °C, 10 h, 95 %; iii) Fe, HCl, 95 °C, 4 h, 71 %; iv) $BrCH_2COOtBu$, DIEA, CH_3CN, 80 °C, 48 h, then LiOH, THF, H_2O, 20 °C, 2 h, 38 % over two steps; v) **3**, HATU, DIEA, CH_2Cl_2, RT, overnight, then CH_3OH, 30 % Pd/C, H_2, RT, 5 h, 40 % over two steps; vi) C_5H_5N, Ac_2O, RT, 24 h, 99 %; vii) Pd/C, H_2, RT, 10 h, 71 %; viii) **6**, HATU, DIEA, CH_2Cl_2, RT, 10 h, then TFA, TIPS, H_2O, CH_2Cl_2, RT, 14 h, 55 % over two steps. DME = dimethyl ether, DIEA = diisopropylethylamine, HATU = (7-azabenzotriazol-1-yl)tetramethyluronium hexafluorophosphate, TFA = trifluoroacetic acid, TIPS = triisopropylsilane.

Experimental data: The method for preparation of paramagnetically labelled lactose is outlined in Scheme 1. For the transformation of **4** to **6**, Scheme 1 summarises two steps in one; however, spectroscopic data are given below for each reaction step. Starting materials were purchased from commercial suppliers and were used without further purification.

4′-Nitro-1,1′-biphenyl-4-carboxylic acid methyl ester (1): [$Pd(PPh_3)_2Cl_2$] (813 mg, 1.15 mmol) was added to a degassed solution of 1-bromo-4-nitrobenzene (4.67 g, 23.2 mmol) in DME (100 mL) and the mixture was stirred for 5 min. Then, methyl-4-boronobenzoate (5.00 g, 27.8 mmol) and aqueous 2 M Na_2CO_3 (30 mL) were added and the mixture was heated to reflux at 90 °C for 5 h.[45] Subsequently, the hot solution was filtered through Celite, cooled, extracted with water and concentrated under reduced pressure. The residue was recrystallised from a 1:1 mixture of ethyl acetate and n-hexane to yield a white solid (4.32 g, 16.1 mmol, 72 %). M.p. 168–170 °C; ^{1}H NMR (400 MHz, [D_6]acetone, 25 °C, TMS): δ = 8.80 (2H; AA′ part of AA′XX′), 8.60 (2H; XX′ part of AA′XX′), 8.49 (2H; AA′ part of AA′XX′), 8.39 (2H; AA′ part of AA′XX′), 3.35 ppm (s, 3H); ^{13}C NMR (100 MHz, [D_6]acetone, 25 °C, TMS): δ = 166.5, 147.6, 146.3, 143.0, 130.5, 130.4, 128.1, 127.4, 124.2, 52.3 ppm; MS (ESI): m/z (%): 279.2 [M+Na]$^+$ (100), 267.3 (11).

4′-Nitro-1,1′-biphenyl-4-carboxylic acid benzyl ester (2): Titanium(IV) isopropoxide (0.7 mL, 2.3 mmol) was added to 4′-nitro-1,1′-biphenyl-4-carboxylic acid methyl ester (**1**, 1.393 g, 5.7 mmol) in a mixture of benzyl alcohol (11.8 mL, 114 mmol) and toluene (90 mL) and the mixture was heated to reflux at 150 °C for 10 h.[46] Then, the solution was allowed to cool to room temperature and was concentrated under reduced pressure, followed by purification on a silica column with n-hexane/ethyl acetate

(5:1) eluent mixture to yield a yellow solid (1.802 g, 5.4 mmol, 95%). ^{1}H NMR (400 MHz, $CDCl_3$, 25°C, TMS): δ = 8.32 (2H; AA′ part of AA′XX′), 8.20 (2H; XX′ part of AA′XX′), 7.76 (2H; AA′ part of AA′XX′), 7.68 (2H; XX′ part of AA′XX′), 7.48–7.36 (m, 5H), 5.40 ppm (s, 2H); ^{13}C NMR (100 MHz, $CDCl_3$, 25°C, TMS): δ = 166.3, 148.0, 146.7, 143.6, 136.3, 130.9, 130.7, 129.2, 128.9, 128.6, 128.5, 127.7, 124.6, 67.3 ppm; MS (ESI): *m*/*z* (%): 334.2 $[M+H]^+$ (100), 242.2 (38); HRMS (ESI): (CH_3OH, NH_4OH, positive mode): *m*/*z* calcd for $C_{13}H_8NO_4$: 242.045334 $[M]^+$; found: 242.0458813.

4′-Amino-1,1′-biphenyl-4-carboxylic acid benzyl ester (3): A mixture of 4′-nitro-1,1′-biphenyl-4-carboxylic acid benzyl ester (**2**, 500 mg, 1.5 mmol) and ethanol was heated to reflux (95°C). After about 10 min, iron powder (837 mg, 0.015 mol) and 1 M aqueous HCl solution (0.95 mL) were added.[47] The mixture was heated at reflux for 4 h, then allowed to cool to room temperature. The iron was removed by filtration through Celite and the filtrate was concentrated under reduced pressure. The residue was diluted with ethyl acetate and purified on a silica column with *n*-hexane/ethyl acetate (2:1) eluent mixture to yield a white solid (455.0 mg, 1.5 mmol, 71%). M.p. 179–180°C; ^{1}H NMR (400 MHz, $CDCl_3$, 25°C, TMS): δ = 8.05 (2H; AA′ part of AA′XX′), 7.60 (2H; XX′ part of AA′XX′), 7.46 (2H; AA′ part of AA′XX′), 6.76 (2H; XX′ part of AA′XX′), 5.38 (s, 2H, $COCH_2$), 3.93 ppm (s, 3H); ^{13}C NMR (100 MHz, [D_6]DMF, 25°C, TMS): δ = 166.7, 150.1, 146.0, 130.0, 127.9, 127.2, 126.6, 125.5, 114.6, 66.9, 51.8 ppm; MS (ESI): *m*/*z* (%): 269.2 $[M+Na^+]$ (49), 228.1 $[M+H^+]$ (100); HRMS (ESI; CH_3OH, NH_4OH, positive mode): *m*/*z* calcd for $C_{20}H_{17}NO_2$: 304.13321 $[M+H]^+$; found: 304.13316.

(*R*)-2,3-Bis[di(*tert*-butoxycarbonylmethyl)amino] propionic acid (4):[15b] *tert*-Butyl bromoacetate (6.83 mL, 9.02 g, 46.2 mmol) was added to a suspension of (*R*)-2,3-diaminopropionic acid hydrochloride (1.00 g, 7.1 mmol), *N*-ethyldiisopropylamine (8.52 mL, 6.44 g, 49.8 mmol) and acetonitrile (50 mL). After heating at reflux for 16 h, additional *tert*-butyl bromoacetate (1.05 mL, 1.39 g, 7.1 mmol) and *N*-ethyldiisopropylamine (1.22 mL, 0.92 g, 7.1 mmol) were added. The reaction mixture was heated at reflux for 32 h, cooled, and the solvent was removed under reduced pressure. The residue was mixed with diethyl ether (100 mL), heated at reflux for 1 h, cooled, and filtered. The filtrate was washed with 0.1 M phosphate buffer of pH 2.0, dried, and concentrated under reduced pressure. The residue was dissolved in tetrahydrofuran (60 mL), and aqueous lithium hydroxide (1 mol dm^{-3}, 7.1 mL, 7.1 mmol) was added. After stirring at room temperature for 3 h, additional aqueous LiOH (1 mol dm^{-3}, 3.6 mL, 3.6 mmol) was added, and stirring was continued for 2 h. Acetic acid (0.63 mL, 0.66 g, 11 mmol) was added and the solvent was removed under reduced pressure. Phosphate buffer (0.1 mol dm^{-3}, pH 2.0, 40 mL) was added and the mixture was extracted with chloroform. The organic phase was dried and concentrated under reduced pressure. The residue was purified on silica gel with chloroform/methanol (10:1) mixture to afford **7** (1.52 g, 2.7 mmol, 38%) as a yellowish oil. NMR and mass spectrometry data were in agreement with the literature.

4′-({(*R*)-2,3-Bis[di(*tert*-butoxycarbonylmethyl)amino]propionyl}amino)-1,1′-biphenyl-4-carboxylic acid benzyl ester (5): 4′-Amino-1,1′-biphenyl-4-carboxylic acid benzyl ester (**3**, 200 mg, 0.66 mmol), HATU, 1-[bis(dimethylamino)-methyliumyl]-1*H*-1,2,3-triazolo[4,5-*b*]pyridine-3-oxide hexafluorophosphate (300 mg, 0.79 mmol) and (*R*)-2,3-bis[di(*tert*-butoxycarbonylmethyl)amino]propionic acid (440 mg, 0.79 mmol) were dissolved in a mixture of dichloromethane (8 mL) and *N*-ethyldiisopropylamine (0.57 mL, 3.3 mmol).[48] The reaction was allowed to run overnight, then the mixture was extracted with 0.1 M aqueous HCl, concentrated and the residue was purified on a silica gel column with *n*-hexane/ethyl acetate (5:1) as eluent, to yield a yellowish oil (523.4 mg, 0.62 mmol, 94%). ^{1}H NMR (400 MHz, $CDCl_3$, 25°C, TMS): δ = 8.11 (2H; AA′ part of AA′XX′), 7.80 (2H; XX′ part of AA′XX′), 7.64 (2H; AA′ part of AA′XX′), 7.58 (2H; XX′ part of AA′XX′), 7.46 (2H; A of ABC), 7.31–7.43 (3H; B and C of ABC), 5.38 (s, 2H), 3.74 (dd, ^3J(H,H) = 5.6, 7.6 Hz, 1H), 3.55–3.62 (m, 6H), 3.47 (d, ^3J(H,H) = 17.0 Hz, 1H), 3.42 (d, ^3J(H,H) = 17.0 Hz, 1H), 3.37 (dd, ^3J(H,H) = 5.6, 14.0 Hz, 1H), 3.0 (dd, ^3J(H,H) = 7.6, 14.0 Hz, 1H), 1.46–1.43 ppm (m, 36H); ^{13}C NMR (100 MHz, $CDCl_3$, 25°C, TMS): δ = 172.1 (2C), 171.8, 171.1 (2C), 166.8, 145.8, 139.4, 136.6, 135.2, 130.6, 129.0, 128.7, 128.6, 128.5, 128.0, 127.0, 120.2, 81.7, 81.5, 67.0, 65.4, 60.8, 56.9, 54.8, 54.7, 28.6, 28.5, 28.4, 28.3 ppm; MS (ESI): *m*/*z* (%): 1693.1 $[2M+H]^+$ (9), 846.6 $[M+H]^+$ (100), 622.3 (73).

4′-({(*R*)-2,3-Bis[di(*tert*-butoxycarbonylmethyl)amino]propionyl}amino)-1,1′-biphenyl-4-carboxylic acid (6): 4′-({(*R*)-2,3-Bis-[di(*tert*-butoxycarbonylmethyl)-amino]propionyl}amino)-1,1′-biphenyl-4-carboxylic acid benzyl ester (236.0 mg, 0.28 mmol) was dissolved in methanol (10 mL) and Pd on charcoal (30%, 5 mg) was added. The mixture was hydrogenated at atmospheric pressure for 5 h, then it was filtered through Celite and concentrated under reduced pressure. The residue was purified on a silica gel column with chloroform/methanol (10:1) eluent mixture to yield a yellow solid (90.6 mg, 0.12 mmol, 43%). ^{1}H NMR (400 MHz, $CDCl_3$, 25°C, TMS): δ = 8.17 (2H; AA′ part of AA′XX′), 7.83 (2H; XX′ part of AA′XX′), 7.69 (2H; AA′ part of AA′XX′), 7.61 (2H; XX′ part of AA′XX′), 3.78 (t, ^3J(H,H) = 6.08 Hz, 1H), 3.58–3.65 (m, 6H), 3.38–3.53 (m, 3H), 3.03 (dd, ^3J(H,H) = 7.9, 14.1 Hz, 1H), 1.46–1.43 ppm (m, 36H); ^{13}C NMR (100 MHz, $CDCl_3$, 25°C, TMS): δ = 171.7 (4C), 171.0, 145.9, 139.0, 134.8, 130.7(2C), 127.7, 127.6 (2C), 126.6 (2C), 119.8 (2C), 81.4 (4C), 56.4, 54.4, 49.5, 30.6 ppm (12C); HRMS (ESI): (CH_3OH, NH_4OH, positive mode): *m*/*z* calcd for $C_{20}H_{17}NO_2$: 756.40659 $[M+H]^+$, 778.38853 $[M+Na]^+$; found: 756.40669, 778.38858.

1-Azido-1-deoxy-hepta-*O*-acetyl-β-D-lactopyranoside (7): 1-Azido-1-deoxy-β-D-lactopyranoside (500 mg, 1.4 mmol) was dissolved in pyridine (15 mL) and acetic anhydride was added (4.5 mL, 47.7 mmol). The mixture was stirred for 24 h, then extracted with chloroform and 1 M aqueous HCl five times. The organic phase was filtered through $MgSO_4$ and concentrated under reduced pressure to give a white solid (918. 2 mg, 1.39 mmol, 99%). ^{1}H NMR (400 MHz, $CDCl_3$, 25°C, TMS): δ = 5.35 (d, ^3J(H,H) = 3.4 Hz, 1H), 5.21 (t, ^3J(H,H) = 9.2 Hz, 1H), 5.11 (dd, ^3J(H,H) = 7.9, 10.4 Hz, 1H), 4.96 (dd, ^3J(H,H) = 3.4, 10.4 Hz, 1H), 4.87 (t, ^3J-(H,H) = 9.0 Hz, 1H), 4.63 (d, ^3J(H,H) = 9.0 Hz, 1H), 4.51 (dd, ^3J(H,H) = 1.9, 10.5 Hz, 1H), 4.49 (dd, ^3J(H,H) = 5.0, 7.9 Hz, 1H), 4.06–4.18 (m, 3H), 3.89 (dd, ^3J(H,H) = 7.2, 1.9 Hz, 1H), 3.82 (t, ^3J(H,H) = 9.0 Hz, 1H), 3.71 (ddd, ^3J(H,H) = 1.9, 5.0, 11.8 Hz, 1H), 2.15 (s, 3H), 2.13 (s, 3H), 2.07 (s, 3H), 2.06 (s, 3H), 2.052 (s, 3H), 2.051 (s, 3H), 1.97 ppm (s, 3H); ^{13}C NMR (100 MHz, $CDCl_3$, 25°C, TMS): δ = 174.6, 170.3, 170.1, 170.0, 169.6, 169.5, 169.1, 101.1, 87.6, 75.7, 74.7, 72.5, 71.0, 70.9, 70.7, 69.0, 66.5, 61.7, 60.7, 21.2 (2C), 20.8, 20.7, 20.6 (2C), 20.4 ppm; MS (ESI): *m*/*z* (%): 741.3 $[M+$pyridine$]^+$ (80), 619.2 (20), 331.1 (100).

1-Amino-1-deoxy-hepta-*O*-acetyl-β-D-lactopyranoside (8): 1-Azido-1-deoxy-hepta-*O*-acetyl-β-D-lactopyranoside (67.8 mg, 0.103 mmol) was dissolved in methanol (5 mL), Pd on charcoal (2 mg) was added and the mixture was hydrogenated for 10 h at atmospheric pressure. The mixture was filtered through Celite and concentrated under reduced pressure to give a colourless oil (46.3 mg, 0.073 mmol, 71%). ^{1}H NMR (400 MHz, $CDCl_3$, 25°C, TMS): δ = 5.34 (d, ^3J(H,H) = 2.8 Hz, 1H), 5.20 (t, ^3J-(H,H) = 9.2 Hz, 1H), 5.08 (dd, ^3J(H,H) = 8.0, 10.4, 1H), 4.95 (dd, ^3J-(H,H) = 3.6, 10.4 Hz, 1H), 4.73 (t, ^3J(H,H) = 9.2 Hz, 1H), 4.4–4.55 (m, 2H), 4.03–4.18 (m, 4H), 3.84 (brt, ^3J(H,H) = 6.4 Hz, 1H), 3.67 (dd, ^3J-(H,H) = 9.6, 18 Hz, 1H), 3.60 (dd, ^3J(H,H) = 3.2, 10.0 Hz, 1H), 2.15 (s, 3H), 2.12 (s, 3H), 2.06 (s, 12H), 2.05 (s, 3H), 1.96 ppm (s, 3H); ^{13}C NMR (100 MHz, $CDCl_3$, 25°C, TMS): δ = 172.1 (2C), 170.5, 170.4, 170.3, 170.1, 170.0, 169.6, 169.0, 101.0, 84.6, 76.6, 73.6, 72.9, 72.4, 70.9, 70.6, 69.1, 66.6, 62.3, 60.8, 20.8, 20.7, 20.5 (4CH_3), 20.4 ppm; MS (ESI): *m*/*z* (%): 636.3 $[M+H]^+$ (100), 576.3 (30), 331.3 (18).

Sugar tag (9): 1-Amino-1-deoxy-hepta-*O*-acetyl-β-D-lactopyranoside (65.2 mg, 0.1 mmol), 4′-({(*R*)-2,3-bis[di(*tert*-butoxycarbonylmethyl)amino]propionyl}amino)-1,1′-biphenyl-4-carboxylic acid (86.8 mg, 0.1 mmol), HATU (58.5 mg, 0.15 mmol) and *N*-ethyldiisopropylamine (87 μL, 0.5 mmol) were dissolved in dichloromethane (5 mL) and the mixture was stirred for 10 h.[48] The mixture was then purified on a silica gel column with chloroform/methanol (10:1) eluent mixture to yield the *tert*-butoxycarbonyl (Boc) and *t*Bu-protected sugar. HRMS (ESI; CH_3OH, NH_4OH, positive mode): *m*/*z* calcd for $C_{66}H_{92}N_4O_{27}$: 1373.60217 $[M+H]^+$; found: 1373.60245. The protected sugar (107 mg, 0.093 mmol) was dissolved in dichloromethane (10 mL), and triisopropylsilane (0.3 mL, 0.72 mmol) and water (2 drops) were added followed by the addition of TFA (1.0 mL, 12.9 mmol) and the mixture was stirred at ambient temperature for 14 h. Following neutralisation with aqueous NaOH (1.0 M), the

mixture was concentrated under reduced pressure (94.9 mg). The crude product was then dissolved in a mixture of CD_3OD and D_2O and transferred into an NMR tube. Small aliquots of 40% NaOD in D_2O were added until the disappearance of the methyl signals of the acetyl protecting groups. The solution was neutralised and concentrated under reduced pressure. The crude product was purified by HPLC, and the pure fractions were lyophilised (44.0 mg, 0.051 mmol, 55%). ^{1}H NMR (900 MHz, D_2O, 25 °C, TMS): δ = 7.85 (2H; AA′ part of AA′XX′), 7.72 (2H; XX′ part of AA′XX′), 7.66 (2H; AA′ part of AA′XX′), 7.50 (2H; XX′ part of AA′XX′), 5.17 (d, ^3J(H,H) = 9.3 Hz, 1H; Glu-H1), 4.41 (t, ^3J(H,H) = 7.8 Hz, 1H; Gal-H1), 3.89 (dd, ^3J(H,H) = 11.0, 12.9, 1H; Glu-H6a), 3.86 (dd, ^3J(H,H) = 2.8, 3.2 Hz, 1H; Gal-H4), 3.78 (dd, ^3J(H,H) = 2.3, 12.9 Hz, 1H; Glu-H6b), 3.74 (dd, ^3J(H,H) = 2.4, 11.3 Hz, 1H; Tag-CH), 3.74 (dd, ^3J(H,H) = 10.0, 10.6 Hz, 1H; Gal-H6a), 3.73 (dd, ^3J(H,H) = 10.0, ^2J(H,H) = 16.0 Hz, 2H; Tag-CH_2), 3.73 (dd, ^3J(H,H) = 9.9, 11.3 Hz, 1H; Gal-H6b), 3.70 (dd, ^3J(H,H) = 9.9, 11.0 Hz, 1H; Glu-H4), 3.69 (dd, ^2J(H,H) = 16.0 Hz, 8H; Tag-CH_2), 3.68 (ddd, ^3J(H,H) = 2.3, 11.0, 11.0 Hz, 1H; Glu-H5), 3.68 (dd, ^3J(H,H) = 9.6, 11.0 Hz, 1H; Glu-H3), 3.66 (ddd, ^3J(H,H) = 2.8, 9.9, 11.3 Hz, 1H; Gal-H5), 3.59 (dd, ^3J(H,H) = 3.2, 9.8 Hz, 1H; Gal-H3), 3.58 (dd, ^3J(H,H) = 9.3, 9.6 Hz, 1H; Glu-H2), 3.50 ppm (dd, ^3J(H,H) = 7.8,9.8 Hz, 1H; Gal-H2); ^{13}C NMR (225 MHz, D_2O, 25 °C, TMS): δ = 179.3 (COOH), 171.2 (CONH), 170.3 (CONH), 143.9 (C-Ar), 136.9 (C-Ar), 135.3(C-Ar), 131.1 (C-Ar), 128.1 (2CH-Ar), 127.7 (2CH-Ar), 126.9 (2CH-Ar), 122.4 (2CH-Ar), 102.8 (Gal-C1), 79.7 (Glu-C1), 77.7 (Glu-C5), 76.4 (Glu-C4), 75.3 (Gal-C5), 75.0 (Glu-C3), 72.4 (Gal-C3), 71.3 (Glu-C2), 70.9 (Gal-C2), 68.5 (Gal-C4), 60.94 (4×Tag-CH_2), 60.96 (2C, Tag-CH and Tag-CH_2), 60.95 (Gal-C6), 59.8 ppm (Glu-C6); HRMS (ESI; CH_3OH, NH_4OH, negative mode): m/z calcd for $C_{66}H_{92}N_4O_{27}$: 853.26326 $[M-H]^-$; found: 853.26309.

Computational conformation analysis: Conformational searches were performed by using the systematic search method SPMC. The OPLS-2005 all-atom force field was employed as implemented in the program MacroModel 9.02,[21] as this force field provides high-quality stretching, binding and torsion parameters for the investigated compounds.[19] The GB/SA method developed by Still[20] was employed. The number of torsion angles allowed to vary during each Monte Carlo step ranged from 1 to $n-1$ for which n equals the total number of rotatable bonds. Amide bonds were fixed in the *trans* configuration. Twenty thousand Monte Carlo steps were performed followed by 2×10000 PR conjugate gradient minimisation steps and a cut-off of 0.1 Å was applied; conformations within 41.8 kJmol^{-1} of the global minimum were kept. The available conformational space of free lactose and the tagged lactose were found to be comparable, as shown in Figure S1 (Supporting Information). For the tagged lactose 637 low-energy conformations were found, of which 27 representing the low-energy conformations (L1–L5) previously reported based on adiabatic energy-map calculations[5] were selected. Overlap of the free and tagged lactose conformations as a function of the Ψ and ϕ angles are shown in Figure S1. To avoid over-fitting, 27 geometries representative of the low-energy regions of the potential energy map were selected out of 637 conformations generated.

Acknowledgements

This work was supported by the Max Planck Society (to C.G.) and the Swedish Research Council (2004-3073, 2007-4407 to M.E.). A.N.V thanks Spanish Ministerio de Ciencia e Innovación for a "Ramón y Cajal" research contract and Xunta de Galicia/FEDER (Consellería de Educación 2009/071) for financial support.

[1] K. Kornfeld, M. L. Reitman, *J. Biol. Chem.* **1981**, *256*, 6633.
[2] a) T. Zhuang, H.-S. Lee, B. Imperiali, J. Prestegard, *Protein Sci.* **2008**, *17*, 1220; b) R. A. Dwek, *Chem. Rev.* **1996**, *96*, 683.
[3] J. M. Alonso-Plaza, M. A. Canales, M. Jimenez, J. L. Roldán, A. García-Herrero, L. Iturrino, J. L. Asensio, J. F. Cañada, A. Romero, H.-C. Siebert, S. André, D. Solís, H.-J. Gabius, J. Jiménez-Barbero, *Biochim. Biophys. Acta Gen. Subj.* **2001**, *1568*, 225.
[4] a) L. L. Houston, T. P. Dooley, *J. Biol. Chem.* **1982**, *257*, 4147; b) E. Rutenber, J. D. Robertus, *Proteins: Struct. Funct. Genet.* **1991**, *10*, 260.
[5] J. Oh, Y. Kim, Y. Won, *Bull. Korean Chem. Soc.* **1995**, *16*, 1153.
[6] K. Hirotsu, A. Shimada, *Bull. Chem. Soc. Jpn.* **1974**, *47*, 1872.
[7] J. H. Noordik, P. T. Beurskens, P. Bennema, R. A. Visser, R. O. Gould, *Z. Kristallogr.* **1984**, *168*, 59.
[8] V. L. Bevilacqua, D. S. Thomson, J. H. Prestegard, *Biochemistry* **1990**, *29*, 5529.
[9] M. Martín-Pastor, A. Canales, F. Corzana, J. L. Asensio, J. Jiménez-Barbero, *J. Am. Chem. Soc.* **2005**, *127*, 3589.
[10] D. I. Freedberg, S. O. Ano, S. E. Norris, R. M. Venable, *NMR Spectroscopy and Computer Modeling of Carbohydrates*, ACS, New York, **2006**, Chapter 12, p. 220.
[11] D. O. Cicero, G. Barbato, R. Bazzo, *J. Am. Chem. Soc.* **1995**, *117*, 1027.
[12] D. A. Cumming, J. P. Carver, *Biochemistry* **1987**, *26*, 6664.
[13] C. L. Perrin, *Science* **1994**, *266*, 1665.
[14] a) X. Xu, P. H. J. Keizers, W. Reine, F. Hannemann, R. Bernhardt, M. Ubbink, *J. Biomol NMR* **2009**, *43*, 247; b) I. Bertini, C. Luchinat, G. Parigi, R. Pierattelli, *Dalton Trans.* **2008**, 3782.
[15] a) P. Haberz, F. F. Rodríguez-Castañeda, J. Junker, S. Becker, A. Leonov, C. Griesinger, *Org. Lett.* **2006**, *8*, 1275; b) A. Leonov, B. Voigt, F. Rodríguez-Castañeda, P. Sakhaii, C. Griesinger, *Chem. Eur. J.* **2005**, *11*, 3342.
[16] T. Ikegami, L. Verdier, P. Sakhaii, S. Grimme, B. Pescatore, K. Saxena, K. M. Fiebig, C. Griesinger, *J. Biomol. NMR* **2004**, *29*, 339.
[17] F. Rodriguez-Castañeda, P. Haberz, A. Leonov, C. Griesinger, *Magn. Reson. Chem.* **2006**, *44*, S10.
[18] W. L. Jorgensen, D. S. Maxwell, J. Tirado-Rives, *J. Am. Chem. Soc.* **1996**, *118*, 11225.
[19] C. A. Stortz, G. P. Johnson, A. D. French, G. I. Csonka, *Carbohydr. Res.* **2009**, *344*, 2217.
[20] W. C. Still, A. Tempczyk, R. C. Hawley, T. Hendrickson, *J. Am. Chem. Soc.* **1990**, *112*, 6127.
[21] F. Mohamadi, N. G. J. Richards, W. C. Guida, R. Liskamp, M. Lipton, C. Caufield, G. Chang, T. Hendrickson, W. C. Still, *J. Comput. Chem.* **1990**, *11*, 440.
[22] a) L. E. Kay, P. Keifer, T. Saarinen, *J. Am. Chem. Soc.* **1992**, *114*, 10663; b) E. Kupče, R. Freeman, *J. Magn. Reson.* **2007**, *187*, 258; c) A. G. Palmer III, J. Cavanagh, P. E. Wright, M. Rance, *J. Magn. Reson.* **1991**, *93*, 151; d) J. Schleucher, M. Schwendinger, M. Sattler, P. Schmidt, O. Schedletzky, S. J. Glaser, O. W. Sorensen, C. Griesinger, *J. Biomol. NMR* **1994**, *4*, 301.
[23] I. Bertini, M. B. L. Janik, Y.-M. Lee, C. Luchinat, A. Rosato, *J. Am. Chem. Soc.* **2001**, *123*, 4181.
[24] a) E. J. d′Auvergne, P. R. Gooley, *J. Biomol. NMR* **2008**, *40*, 107; b) E. J. d′Auvergne, P. R. Gooley, *J. Biomol. NMR* **2008**, *40*, 121.
[25] a) M. L. Sinnott, *Carbohydrate Chemistry and Biochemistry*, RSC, Cambridge, **2007**, p. 50; b) M. Miljkovic, *Carbohydrates, Synthesis Mechanisms and Stereoelectronic Effects*, Springer, Heidelberg, **2010**, p. 41.
[26] M. Zweckstetter, *Nat. Protocols* **2008**, *3*, 679.
[27] H. Akaike, *IEEE Trans. Autom. Control* **1974**, *19*, 716.
[28] W. Zucchini, *J. Math. Psychol.* **2000**, *44*, 41.
[29] E. J. d′Auvergne, P. R. Gooley, *J. Biomol. NMR* **2003**, *25*, 25.
[30] a) L. Poppe, R. Stuike-Prill, B. Meyer, H. Van Halbeek, *J. Biomol. NMR* **1992**, *2*, 109; b) J.-F. Espinosa, H. Dietrich, M. Martín-Lomas, R. R. Schmidt, J. Jiménez-Barbero, *Tetrahedron Lett.* **1996**, *37*, 1467.
[31] L. Verdier, P. Sakhaii, M. Zweckstetter, C. Griesinger, *J. Magn. Reson.* **2003**, *163*, 353.
[32] In-phase/anti-phase (IPAP)–HSQC provides clear ^1J doublets and is often used for ^{1}H,^{15}N RDC and PCS measurements for proteins so its application was therefore attempted. It allows for measurement of RDCs in the less resolved ^{13}C dimension and hence its use did not result in reduced measurement errors. Due to the noisiness of these data, the IPAP–HSQC information was not used in this study.

[33] a) L. Poppe, H. Van Halbeek, *Magn. Reson. Chem.* **1993**, *31*, 665; b) S. Hesse, C, Jäger, *Cellulose* **2005**, *12*, 5.
[34] G. Otting, *Annu. Rev. Biophys.* **2010**, *39*, 387.
[35] N. Nevins, D. Cicero, J. P. Snyder, *J. Org. Chem.* **1999**, *64*, 3979.
[36] A. R. Leach, *Molecular Modelling, Principles and Applications*, Addison Wesley Longman, Edinburgh, **1998**, p. 414.
[37] D. K. Agrafiotis, A. C. Gibbs, F. Zhu, S. Izrailev, E. Martin, *J. Chem. Inf. Model.* **2007**, *47*, 1067.
[38] P. Bonnet, D. K. Agrafiotis, F. Zhu, E. Martin, *J. Chem. Inf. Model.* **2009**, *49*, 2242.
[39] M. Erdélyi, B. Pfeiffer, K. Haunstein, J. Fohrer, J. Gertsch, K. H. Altmann, T. Carlomagno, *J. Med. Chem.* **2008**, *51*, 1469.
[40] H. Andersson, H. Demaegdt, G. Vauquelin, G. Lindeberg, A. Karlén, M. Hallberg, M. Erdelyi, A. Hallberg, *J. Med. Chem.* **2010**, *53*, 8059.
[41] a) D. Altschuh, O. Vix, B. Rees, J. C. Thierry, *Science* **1992**, *256*, 92; b) J. Jiménez-Barbero, A. Canales, P. T. Northcote, R. M. Buey, J. M. Andreu, J. F. Díaz, *J. Am. Chem. Soc.* **2006**, *128*, 8757; c) P. Thepchatri, T. Eliseo, D. O. Cicero, D. Myles, J. P. Snyder, *J. Am. Chem. Soc.* **2007**, *129*, 3127.
[42] S. Yamamoto, T. Yamaguchi, M. Erdelyi, C. Griesinger, K. Kato, *Chem. Eur.J.* **2011**, DOI: chem.201100856.
[43] F. Tian, H. M. Al-Hashimi, J. L. Craighead, J. H. Prestegard, *J. Am. Chem. Soc.* **2001**, *123*, 485.
[44] a) M. Ottiger, F. Delaglio, A. Bax, *J. Magn. Reson.* **1998**, *131*, 373; b) A. Garza-García, G. Ponzanelli-Velázquez, F. Del Río-Portilla, *J. Magn. Reson.* **2001**, *148*, 214.
[45] a) R. Frenette, R. W. Friesen, *Tetrahedron Lett.* **1994**, *35*, 9177; b) Y. Matsushita, K. Sakamoto, T. Murakami, T. Matsui, *Synth. Commun.* **1994**, *24*, 3307.
[46] G. Shapiro, M. Marzi, *J. Org. Chem.* **1982**, *62*, 7096.
[47] J. T. Roland, Z. Guan, *J. Am. Chem. Soc.* **2004**, *126*, 14328.
[48] M. Erdélyi, V. Langer, A. Karlén, A. Gogoll, *New J. Chem.* **2002**, *26*, 834.

Received: March 20, 2011
Published online: July 13, 2011

